ELSEVIER

Influence of mixing methods on the NO_x reduction capability and electrical properties of photocatalytic cementitious systems

Oğuzhan Şahin [a], Samed Bay [b], Hüseyin İlcan [b], Gürkan Yıldırım [b], Mustafa Şahmaran [b,*]

[a] Department of Civil Engineering, Kırşehir Ahi Evran University, Kırşehir, Turkey
[b] Department of Civil Engineering, Hacettepe University, Ankara, Turkey

ARTICLE INFO

ABSTRACT

Nitrogen oxides (NO_x), regarded as toxic air pollutants, are a group of highly reactive and hazardous gases encompassing compounds ranging from nitrous to nitric acid. Especially in crowded cities, the release of these gases from the industrial organizations and vehicles has reached serious levels. To eliminate the adverse effects of these gases, titanium dioxide (TiO_2) is used worldwide as a photocatalyst due to its high efficiency in oxidization of NO_x. Incorporating TiO_2 into cement-based composites gives them photocatalytic capability: uniform and stable dispersion of TiO_2 throughout the matrix is an undisputable requirement for improved photocatalytic efficiency. The main purpose of this study is to investigate the effects of different mixing techniques and surfactant materials on the dispersion of high dosage nano-TiO_2 particles (5% of total weight of binder materials) throughout cement-based materials, with the goal of producing cost-effective cementitious systems, more feasible mixing methods, and ensuring proper dispersion of nano-TiO_2. Five different mixing methods were proposed to achieve uniform distribution of the nano-TiO_2. They were each implemented using different mixing procedures, equipment and surfactants. The performance of each mixing method was evaluated based on photocatalytic performance, electrical impedance (EI), compressive strength and microstructural analysis. Test results showed evidence of the significantly positive effect of polyacrylic acid (PAA) on the dispersion of nano-TiO_2. In general, the highest dispersion occurred with ultrasonication and binary utilization of polycarboxylate ether-based plasticizer (PCE) and PAA. The EI test was a highly effective evaluation method for homogeneous distribution of conductive nano particles throughout the matrix. Results also showed a significant relationship between electrical performance and nitric oxide (NO) degradation of composites, and electrical properties of composites are able to provide a reliable estimate of the photocatalytic efficiency of them.

1. Introduction

Using nano-scale materials has become widespread in various industries over the last few decades due to their ability to improve the properties of conventional materials according to the needs of specific sectors. The abilities of nano materials are of particular interest to the researchers and construction sector, which is focused heavily on construction materials. This attention has led to a number of studies about the nano material incorporation in cement-based systems, with the goal of producing more durable, high-performance and/or environmentally friendly composites. Including air purification capability to cement-based composites by using nano materials is one of the innovative approaches, which allows them to absorb or transform deleterious particles (impurities) in the air. In this regard, researchers have intensified their efforts to develop innovative composites containing nano materials to eliminate or reduce volatile organic compounds sustained in the air such as carbon monoxide, sulfur oxides and nitrogen oxides (NO_x) [1–8].

With the contribution of nitrogen oxides ("NO_x" [NO and NO_2]) to the formation of ozone gases and acid rain, and human health concerns [9,10], using NO_x-reducing materials in concrete technology is gaining more importance. Materials such as titanium dioxide (TiO_2) have been frequently used as a photocatalyst due to their high efficiency in oxidization of NO_x gases [11,12]. TiO_2 shows superior skill in the activation of photocatalytic reactions [13] and due to its chemical/photochemical stability, chemical inertness in the absence of ultraviolet (UV) irradiation, safety, cost-efficiency, and non-toxicity in cement-based systems, it is a suitable photocatalyst [12,14,15]. The photocatalytic activity of semiconductor TiO_2 is highly dependent on the size, shape, type and

phase of the material and changes with particle properties [16]. Due to the high photocatalytic efficiency of nano-sized TiO_2 particles compared to larger size TiO_2 particles [17–22], TiO_2 is generally used at nano-scale in cement-based composites.

The agglomeration of nano materials including nano-TiO_2 is a general problem. This is caused due to intense surface interactions of nano materials, which is triggered by high surface area/energy and very strong attractive forces among nano-sized particles causing difficulties in dispersing them homogeneously throughout the cement-based systems [23] and therefore, their use is limited in cement-based composites [24–26]. Uniform and robust dispersion of nanoparticles is indisputable for their successful and effective use [23]. In photocatalytic cement-based systems incorporating TiO_2, enabling homogenous and effective UV radiation and uniform distribution of TiO_2 particles (especially at nano-scale) along the surface of cement-based composites are some of the main goals to achieve optimum photocatalytic performance. Since the agglomeration problem reduces the photocatalytic activity [27,28], proper dispersion of nano-TiO_2, which is also prone to excessive agglomeration [28,29], is critically important for the production of cement-based composites with high photocatalytic activity.

To uniformly disperse nano materials in an aqueous suspension, ultrasonication and utilization of surfactants are some of the commonly used methods in the literature. For example, Sato et al. [30] investigated the dispersion and agglomeration characteristics of nano and sub-micro scale TiO_2 particles in a suspension (with 15% solid content) prepared by using three different mechanical dispersion agitations and poly acrylic acid (PAA), as a polymer dispersant, with different average molecular weights. They stated that proper dispersion of nano particles is very important to fully benefit from their advantages and ultrasonic irradiation is an effective method to disperse nano particles in aqueous suspensions. Othman et al. [31] examined the effect of different parameters including ultrasonication amplitude/type, and utilization rate of dispersants on the dispersion and stability of photocatalytic nano-TiO_2 particles in aqueous suspensions. They used PAA and ammonium polymethacrylate as different dispersants and their TiO_2 utilization rate was ~0.05% by weight of water. The study concluded that increment in the ultrasonication amplitude has an improving effect on the deagglomeration process and stability of the suspensions. Yousefi et al. [32] studied the effect of various parameters such as concentrations of nano-TiO_2 powder, type of dispersant (lime-saturated water solution and deionized water), mixing process and ultrasonication time on the dispersibility of TiO_2 particles incorporated (up to ~1% by weight of cement) into the cement paste and found that the conventional mixing causes high agglomeration of nano-TiO_2 while ultrasonication is undeniably better in uniformly dispersing nano-TiO_2 throughout the cementitious system. They also stated that utilization of saturated lime water improves the photocatalytic degradation capability of nano-particles as well as convenient dispersion of nano-TiO_2 in cement paste. Sobolkina et al. [26] studied the effects of sonication on the dispersibility of carbon nanotubes (CNTs) in water by considering different implementation periods, types of surfactants (anionic sodium dodecyl sulfate and nonionic polyoxyethylene (23) lauryl ether) with different utilization rates. They also investigated the modification of cement pastes with the CNT-dispersed (up to 0.25%, by weight of cement) solutions. According to their results, a CNT-to-surfactant ratio of 1:1–1:1.5 and a sonication time of 120 min provided the most favorable dispersion. Mendoza et al. [33] investigated the effect of superplasticizer and $Ca(OH)_2$ on the dispersion stability of multi-walled CNTs for cement-based systems with suspensions incorporating 0.25%wt of multi-walled CNTs and concluded that the use of a dispersing agent with the sonication is necessary to ensure a greater degree of dispersion of particles for a longer duration. Alrekabi et al. [34] investigated the dispersion of multi-walled CNTs in water under various sonication conditions to prepare homogeneous suspensions (having different CNT dosages up to 0.05% by weight of cement) for use in the preparation of cementitious composites. They also used superplasticizer to achieve better dispersion of multi-walled CNTs. As a result, they revealed that higher sonication intensity can increase the dispersion level of the suspension and superplasticizer utilized in combination with ultra-sonication provides better distribution of CNTs in water. Saafi et al. [35] also used superplasticizer as a surfactant and ultrasonication as a mixing method to ensure proper dispersion of multi-walled CNTs (up to 1.0% of the total weight of the matrix) in solution prepared for the production of geopolymeric nano-composites. They stated that the nanocomposites produced by using multi-walled CNT concentration 0.1 and 0.5% showed a good dispersion. Yazdani and Mohanam [36] examined the effect of the dosage rate of carbon nano materials (CNT and Carbon Nanofibers (CNF)) (up to 0.2%wt of cement) and water-cement ratio (0.35–0.50) on the various properties of cement mortar reinforced with these nano materials and they used ultrasonication and a surfactant (plasticizer) to ensure a homogeneous mixing. They revealed that nano particles were dispersed uniformly in the aqueous medium by using ultrasonication although proper dispersion was not ensured when mixed with the cement due to re-agglomeration of particles in cement matrices because of absorption of water by the cement. Zhang et al. [37] and Zhang and Islam [38] also used ultrasonication and mechanical mixing to produce cement paste, mortar and concrete specimens incorporating nano silica (2.0%, by the mass of cementitious materials), and stated that ultrasonication provides better dispersion of nano-silica than mechanical mixing. As above-detailed, several researchers have used ultrasonication and/or different surfactants to solve the agglomeration problem of nano particles and improve the dispersion quality. Although higher number of studies has been carried out for the homogeneous dispersion of low-dosage nano materials in cementitious systems, there is very limited number of studies on the homogeneous distribution of high-dosage nano materials. The dispersion of high-dosage nano particles in cement-based systems by using common mixing processes (e.g. ultrasonication) can be quite difficult and even with the very proper dispersion of particles, additional treatments can be required to keep them in the suspended condition, as they tend to re-agglomerate [39–41].

To improve processing methodologies and further evaluate their influence, more research is needed to better understand the mechanisms underlying the effects of mixing methods on the photocatalytic activity and mechanical properties of cement-based composites containing high-dosage nano materials (specifically nano-TiO_2). The current experimental study was undertaken to address the need for cost-effective/feasible mixing methods that will allow proper dispersion of high-dosage nano-TiO_2 (5%, by the total weight of binder) and ensure its stability for a certain period during the fresh state of cement-based composites. Since, aggregates in mortar/concrete mixtures, due to their comparatively larger size than nano-TiO_2 and cement particles, may break down the nano-TiO_2 agglomerates and lead to better dispersion of agglomerates compared to cement paste mixtures, this study was undertaken by focusing on cement paste mixtures only. For this purpose, five different mixing methods were developed taking the extensively performed literature review and authors' preliminary/past studies [42] into account. These mixing methods were based on three main techniques (i.e. ultrasonication, high-shear hand blender and conventional cement mixer) and implemented with different procedures and surfactant contents. Two surfactant materials were used: polycarboxylic ether-based superplasticizer (PCE) and polyacrylic acid (PAA). To compare the mixing methods, in addition to the evaluation of photocatalytic performance, researchers have recorded the compressive strength and electrical impedance results in an effort to determine the mixing method that will be regarded as more successful in terms of dispersion of nano-TiO_2 throughout the cement-based composites.

2. Materials and mixture proportions

CEM I 52.5R white Portland cement (WPC) complying with EN 197–1 [43] was used as the main binder material for all mixtures.

Chemical composition and physical properties of WPC are provided in Table 1. In order to clearly understand the effect of mixing method on dispersion of nano-sized TiO_2 in the cementitious system, a nano-sized anatase form of TiO_2 was used. Table 2 shows its physical properties. TiO_2 powder used in this study was characterized by using scanning electron microscope (SEM) (Tescan GAIA 3 FIB-SEM operated at 3.0 kV) and X-Ray diffraction measurement (XRD) (Rigaku Ultima-IV diffractometer at 40 kV, within a scan range of $2\theta = 5-55°$ and 30 mA with Cu-Kα ($\lambda = 1.5405$ Å) radiation.). To avoid any misleading results, a true representative sample of powder, weighing a few grams, was taken from the core of the powder batch of nano anatase TiO_2 and was dried overnight in an oven before testing. The SEM micrograph image and XRD pattern of the nano-sized anatase form of TiO_2 are shown in Fig. 1. Considerably small size and extremely rough surface morphology of the nano-TiO_2 particles can be seen from Fig. 1a and the diffraction peak value of 25.4°, that can be seen from Fig. 1b, validated the anatase phase/structure of TiO_2 used in this study [44,45].

Cement paste mixtures were prepared with water to binder ratio (w/b) of 0.35, by weight. The available water in chemical admixtures was also considered during the calculation of the w/b ratio. Tests were performed on a trial batch of cement paste specimens nano-modified with TiO_2 to find the optimum TiO_2 content prior to the experimental stage. NO degradation capabilities were calculated for specimen groups with TiO_2 contents ranging from 1% to 20%. The specimens exhibited considerable different NO degradation capability when the percentages of above 5 wt% (including 5%) of TiO_2 were incorporated. Consequently, the cement paste specimens prepared for the experimental stage contained 5% nano-TiO_2 additions by weight.

Two different surfactant materials including polycarboxylic ether-based superplasticizer (PCE) satisfying minimum requirements of ASTM-C494/C494 M standard [46] and polyacrylic acid (PAA) were used together or separately in dosages ranging from 0.5 to 1% to ensure homogeneity of mixtures and better dispersion of nano-sized TiO_2 powders without endangering other mixture properties. PCE was liquid, containing 40% solid material, with a density of 1.1 kg/l. PAA was a white and milky liquid, containing 48% solid material, with a density of 1.22 kg/l and pH value of 3–4.5.

3. Dispersion techniques of TiO_2 at nano-scale

Due to the agglomeration and sedimentation problem of nano-TiO_2 in suspension, and consequently in fresh cement paste mixtures, different mixing equipments (A Vibra-Cell ultrasonic mixer with a 25 mm probe diameter that can be operated at different amplitudes (0–100%) and energy levels (0–9999 J) (Fig. 2-a), a high-speed kitchen-type hand blender (Fig. 2-b) and a conventional cement mixer (Fig. 2-c)) were implemented under different mixing scenarios alongside with surfactant utilization to determine their effectiveness on the dispersion of nano-TiO_2 particles within the cementitious matrices. Initially, the preliminary studies were undertaken for determination of optimum utilization rates of PCE and PAA admixtures and amplitude and energy input values of ultrasonication process. After that, different mixing methods were proposed by considering outcomes from preliminary studies.

3.1. Determination of suitable mixing parameters for TiO_2 dispersion

Selection of amplitude and energy values during the ultrasonication process:

Optimum amplitude and energy value of the ultrasonic mixing process for more homogeneous dispersion of nano-TiO_2 were determined by comparing the duration of suspended state of nano-TiO_2 particles in the solution. The influence of the ultrasonic mixer amplitude value on the zeta potential of suspension was investigated. For this purpose, solution ingredients were determined based on the nano-TiO_2 and water content of a reference mixture with water-to-binder ratio of 0.35 containing 5% nano-TiO_2 by total weight of binder materials. Therefore, 140 mL water and 20 gr nano-TiO_2 were mixed for 10 min with different amplitude values and constant energy inputs of 1100 J. The zeta potential values of the suspensions for different amplitude values are shown in Fig. 3a. Zeta potential results clearly decreased with increased amplitudes of ultrasonication, which means that high amplitude values provide a significant dispersion of TiO_2 particles, leading to increased suspension stability as a result of more repulsive force application of nanoparticles on each other.

After investigating the effect of different amplitude values on the zeta potential measurement, researchers examined the combined effect of sonication with different amplitude and energy input on suspension stability, using the same solution composition and mixing time. The amplitude and energy input values of this experiment are shown in Table 3.

Solutions prepared with the given mixing parameters were stored under the same environmental conditions during an appropriate suspension period. The suspense state of solutions for different time periods is shown in Fig. 4.

Amplitude and energy input value increments caused remarkable increases in period of suspended state. In the D-1 and D-3 solutions, nano-TiO_2 particles completely precipitated in the first 30 min. However, this was not the case for D-5, which was mixed using ultrasonication, using the same amplitude value with a different energy level. Due to the high energy input of D-5, the nano-TiO_2 did not completely collapse, even after 1 h. Although nano-TiO_2 particles in the D-2 solution collapsed in 30 min with an amplitude of 80%, D-4 and D-6 did not show any precipitation in 1-h period. Due to the sufficient duration of suspended state with optimum energy inputs during the ultrasonic mixing process, amplitude and energy input value of the ultrasonic mixer used for the D-4 solution were used in later stages of the study.

Suitable surfactant materials for uniform distribution of nano-TiO_2 in solution:

This section describes the investigation into the effect of utilization rates of surfactant materials on the zeta potential of the suspension. To this end, the ultrasonic mixer was used at 40% amplitude and 1100 J energy input, and solutions were prepared as described above. 140 mL of water, 20 gr nano-TiO_2 and relevant surfactant materials were mixed for
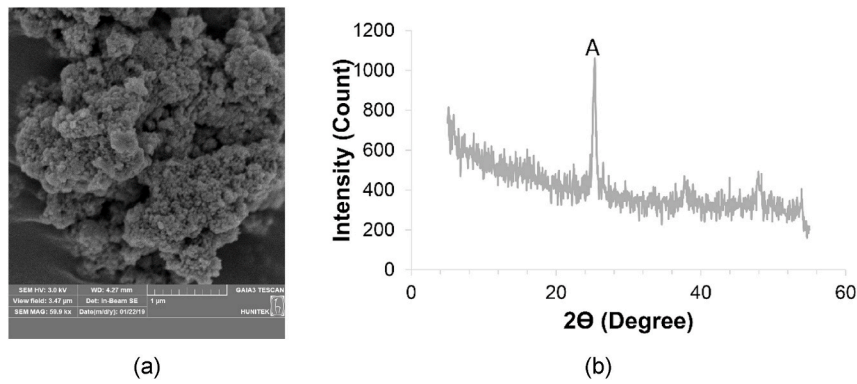
Table 2
Physical properties of Nano Anatase TiO_2.

Physical Properties	Type
	Nano Anatase TiO_2
Purity (%)	99.86
BET[a] (m^2/g)	79.6
Density (gr/cm^3)	3.55
Average Grain Size	10–20 nm
Maximum Grain Size	50 nm
Minimum Grain Size	10 nm

[a] BET: Brunauer–Emmett–Teller surface area.

Table 1
Chemical composition and physical properties of CEM I 52.5R WPC.

Chemical Composition, %							Physical Properties	
SiO_2	Al_2O_3	Fe_2O_3	CaO	MgO	SO_3	Loss of ignition	Density (g/cm^3)	Specific surface, Blaine (cm^2/g)
21.39	3.37	4.89	62.6	2.39	4.55	3.1	3.15	4650

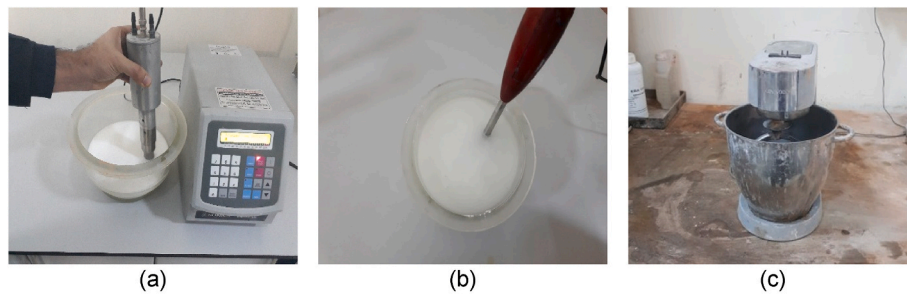**Fig. 1.** (a) SEM micrograph, (b) XRD analysis of nano-sized anatase TiO$_2$.

Fig. 2. The mixing processes of nano sized TiO$_2$ with a) ultrasonic mixer b) high-speed kitchen-type hand blender c) conventional cement mixer.
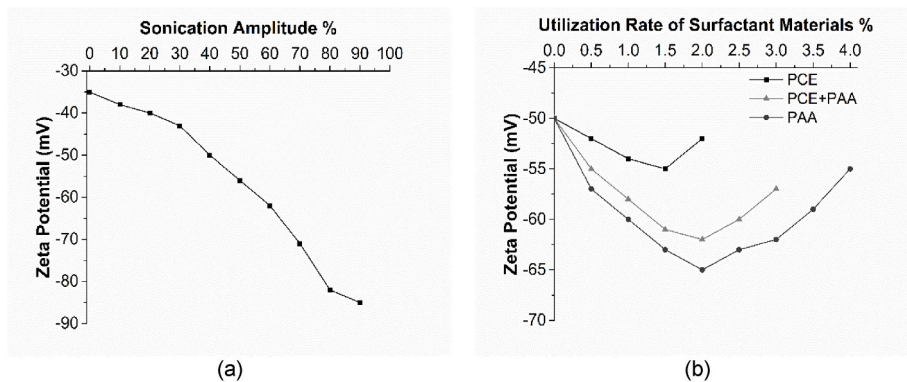

Fig. 3. The influence of (a) sonication amplitude modification, (b) utilization rate of surfactant materials on zeta potential (mV) of suspensions.

Table 3
Amplitude and energy input values of ultrasonic mixer used during mixing process.

Label	Amplitude (%)	Energy (J)
D-1	40	1000 J
D-2	80	1000 J
D-3	40	1900 J
D-4	80	1900 J
D-5	40	4000 J
D-6	80	4000 J

10 min. The effect of PCE on zeta potential was studied with utilization rates of 0.5%, 1%, 1.5% and 2%, by total weight of binder materials. Results in Fig. 3b show that zeta potential value increased negatively up to 1.5% utilization rate of PCE and reached its maximum negative value as −55 mV. Once PCE exceeded 1.5%, a negative decrease started in zeta potential value. Therefore, the optimum utilization rate for PCE in terms of zeta potential was determined as 1.5%. Suspensions including PAA with up to 4% of binder materials by weight were also prepared to evaluate the effect of PAA on zeta potential. Zeta potential value increased negatively up to 2.0% utilization rate of PAA, reaching its maximum value at −65mV, when a negative decrease began (Fig. 3b). With binary utilization of PAA and PCE with equal rates, zeta potential value increased negatively up to 2.0% of total utilization rate of PAA and PCE (1% + 1%), and reached its maximum value at −62mV, when a decrease in negativity started (Fig. 3b). The point of the highest zeta potential value at which the curve changes from a negatively incremental tendency to a negatively decremental direction tendency is where potential stability is highest [31,47]. Therefore, the utilization rate of surfactant for the highest zeta potential values is the optimum value to disperse nano-TiO$_2$ particles throughout the suspensions.

After evaluating zeta potential values according to the surfactant material content of suspensions, solutions with the same composition
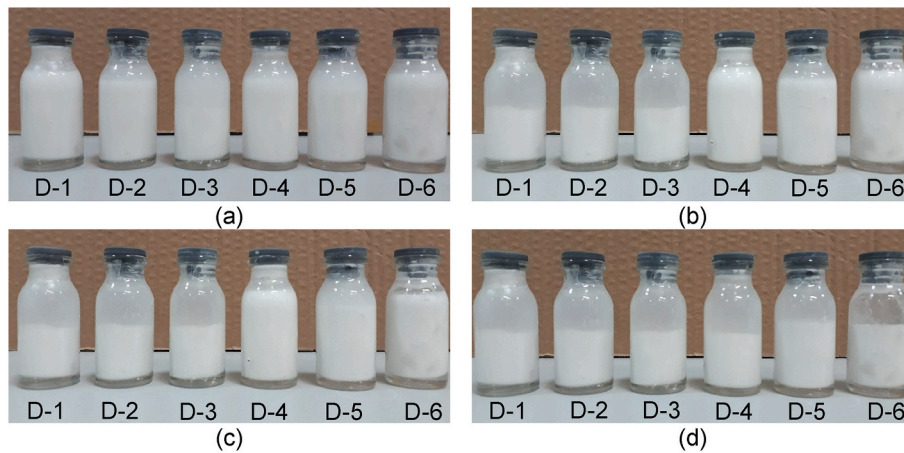
Fig. 4. The dispersion states of nano-TiO$_2$ for different periods a) 15 min, b) 30 min, c) 1 h, d) 2 h..

and mixing time as those used for zeta potential measurements were prepared with different proportions of surfactant materials to examine the effect of the different surfactant contents on the suspended state of TiO$_2$ particles in solutions. Although solutions containing surfactant materials required relatively higher dosages to achieve optimum zeta potential values, using surfactant materials at lower utilization rates can provide sufficient time for sustaining TiO$_2$ dispersion until the final setting time of the concrete. After this time, TiO$_2$ particles can remain scattered as concrete starts to harden. In addition, utilization of surfactant materials affects the hydration process and the mechanical properties of cement-based composites and also raises the cost of production. Taking all these factors into consideration, the utilization rates of surfactant materials seen in Table 4 were determined without compromising the time needed for proper dispersion of TiO$_2$ in cementitious matrices. The prepared solutions were stored under the same environmental conditions, and the precipitation state of TiO$_2$ particles was observed for different periods of time. The precipitation state of solutions for different periods of time and surfactant dosages are displayed in Fig. 5.

The TiO$_2$ particles of S-1 (prepared without surfactant materials) completely precipitated at the bottom of glass jar in a short period. For the S-7 (binary utilization of surfactant materials with 2% utilization rate), the nano-TiO$_2$ did not completely collapse, even after six months. By considering the duration of suspended state of TiO$_2$ particles in regard to single usage of surfactant materials, PAA showed better performance than PCE. Considering both duration of suspended state and zeta potential measurements, optimum utilization rates for single usage were 1% of PCE and 0.5–1% of PAA, separately. In the case of concomitant usage of these surfactant materials, the total optimum utilization rate (equal utilization rate for both) ranged from 1 to 1.5%. With all abovementioned statements taken into account, nano-TiO$_2$ particles were suspended for a sufficient period of time with the concomitant use of 0.5% of PCE and 0.5% of PAA by total weight of powder materials. Nevertheless, in order to clarify the effect in the cement-based mixture, various utilization rates were combined with the

Table 4
Utilization rates of surfactant materials (% by total weight of binder materials).

Label	PCE (%)	PAA (%)
S-1	–	–
S-2	0.5	–
S-3	0.5	0.5
S-4	–	0.5
S-5	1.0	–
S-6	–	1.0
S-7	1.0	1.0

mixing methods described next section.

3.2. Methods for dispersion of nano-TiO$_2$

In light of preliminary studies, five mixing methods were proposed to enhance the dispersion of nano-sized TiO$_2$ and improve photocatalytic performance without endangering the mechanical properties of cement-based matrixes.

1st **mixing method:** This method was used to prepare reference specimens and was a modification of the standard mortar mixing method specified in TS EN 196–1 for the paste phase. All dry raw materials (TiO$_2$ and WPC) were mixed in a 5-L-capacity conventional cement mixer at 100 rpm for 10 min. Mixing water was added into the raw materials over 30 s while mixing was in progress at 100 rpm. Mixing speed was then increased to 300 rpm and all the PCE (1%) was added to the mixer over 30 s. Finally, all the materials were mixed for an additional 10 min at 300 rpm [48].

2nd **mixing method:** TiO$_2$ and PCE (1%) were added to the mixing water and ultrasonication was applied for 10 min with 80% amplitude and 1900 J energy inputs. After ultrasonication, the suspension was slowly added to the WPC in the 5-L-capacity conventional cement mixer operating at 100 rpm over 30 s. Mixing speed was then increased to 300 rpm and mixing was continued for an additional 10 min at 300 rpm [26, 35,49].

3rd **mixing method:** TiO$_2$, PCE (1%) and all of the mixing water were mixed using a hand blender for 10 min at 3000 rpm. After that, the suspension was slowly added to the WPC in the 5-L-capacity conventional cement mixer operating at 100 rpm over 30 s. Mixing speed was then increased to 300 rpm and mixing of all the ingredients (WPC, TiO$_2$, water and PCE) continued for an additional 10 min at 300 rpm.

4th **mixing method:** To evaluate the effect of PAA on the dispersion of TiO$_2$ particles in the cementitious matrices, PAA was used alone by 0.5% of the total weight of powder materials. TiO$_2$ and all of the mixing water were ultrasonicated for 10 min with 80% amplitude and 1900 J energy inputs. PAA was slowly added to this suspension during ultrasonication, then the suspension was slowly added to the WPC in the 5-L-capacity conventional cement mixer operating at 100 rpm over 30 s. Finally, mixing speed was increased to 300 rpm and all the ingredients (WPC, TiO$_2$, water and PAA) were mixed for an additional 10 min at 300 rpm.

5th **mixing method:** PAA and PCE (0.5% + 0.5% of the total weight of powder materials) were used together to evaluate their combined effect on the dispersion of nano-TiO$_2$ particles in cement-based composites. All the ingredients except WPC were ultrasonicated for 10 min with 80% amplitude and 1900 J energy inputs. The suspension obtained at the end of ultrasonication was slowly added to the WPC in the conventional cement mixer operating at 100 rpm over 30 s. As the final step,
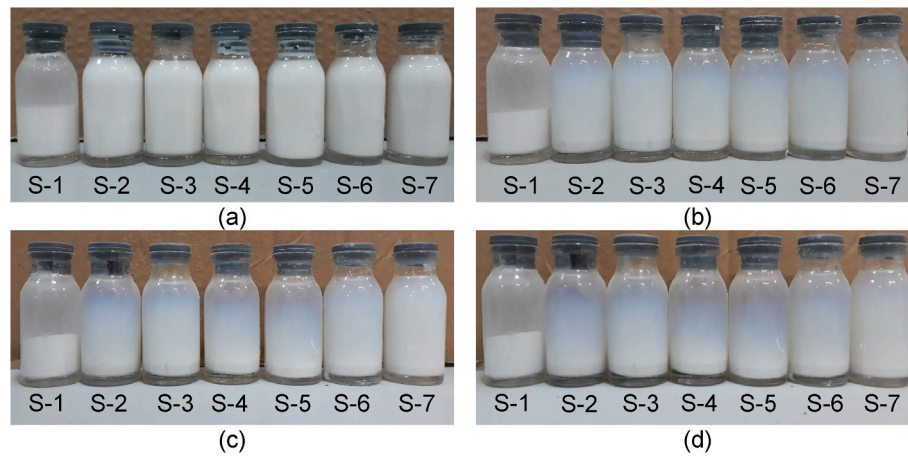
Fig. 5. The dispersion states of nano-TiO$_2$ for different periods a) 2 h, b) 1 month, c) 3 months, d) 6 months.

mixing speed was set to 300 rpm and mixing of all materials (WPC, TiO$_2$, water, PCE and PAA) was continued for an additional 10 min at 300 rpm.

4. Specimen preparation and testing

Mixtures were manufactured by using each proposed mixing method to assess the performance of different mixing methods for dispersion of nano-TiO$_2$ particles by measuring photocatalytic performance, electrical impedance and compressive strength. After mixing, these mixtures were poured into oiled molds and cured in a laboratory environment for 24 h. After initial curing, the specimens were de-molded and further cured in water at room temperature (23 $\pm$ 1 °C) until the time of testing. All mixtures were named with letters and numbers to indicate particle size, TiO$_2$ phase and mixing method. For instance, in mixture NA-3, the TiO$_2$ was nano-anatase, and it was mixed by using the third mixing method.

Compressive strength: The compressive strength test was conducted on 50 mm cubic specimens by following the ASTM C109 standard [50]. Tests were performed at 7 and 28 days under uniaxial loading, at a rate of 0.9 kN/s. Six replicates from each mixing method were tested for each curing age and results were averaged.

Electrical impedance (EI) test: The main purpose of this process is to effectively assess nano-sized TiO$_2$ dispersion capability of the relevant mixing method. Electrical properties of cement-based composites depend on matrix microstructure, and enhanced microstructural homogeneity in cement-based composites containing nano-TiO$_2$ provides a uniform and stable electrical performance throughout the matrix. For EI

measurements of cement-based composites, two Ø100 $\times$ 200 mm cylindrical specimens were prepared using each mixing method. Ø100 $\times$ 50 mm cylinder specimens were extracted from these larger cylinders with a diamond blade. Considering the possibility of inaccuracy in EI measurements due to trowelled and/or molded surface conditions, the top and bottom portion of each specimen were not used to determine electrical property. Consequently, for each mixing method, six Ø100 $\times$ 50 mm-cylindrical pieces were used for EI tests at 7, 28 and 90 days (Fig. 6a) and results were averaged.

A 2-probe electrical resistivity meter – which gives impedance results using alternating current (AC) impedance, works with frequencies from 1 Hz to 30 kHz and detects the phase angle between 0° and 180° – was used to measure EI (Fig. 6b). According to Hou (2008) [51], polarization effect can be eliminated with a frequency of at least 1 kHz AC current application, therefore operating frequency was chosen as 1 kHz for this study. In this configuration, cylindrical specimens were placed between two parallel plate electrodes and wet sponges (10 mm high and 150 mm in diameter) were positioned between the specimen and electrodes to ensure adequate electrical contact. Sponges were each saturated with the same amount of water to eliminate any deflection of the EI measurement results.

Tomography imaging and SEM characterization: The dispersion of nano-TiO$_2$ particles throughout the matrix was also evaluated using a computed tomography device (CT) for non-destructive testing of Ø18 $\times$ 20 mm cylindrical specimens (Fig. 7). Cross-section images from the CT scan were pre-treated for the nano-TiO$_2$ particles to be clearly visible. SEM/EDX (Energy-dispersive X-ray spectroscopy) mapping images,
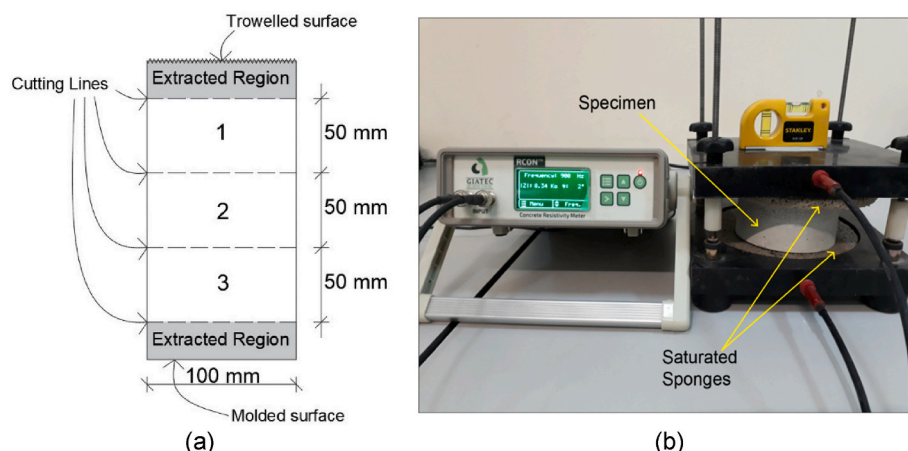

Fig. 6. (a) Specimen preparation, (b) Concrete resistivity meter and testing of a specimen.

Fig. 7. (a) Computed tomography device, (b) test specimens (Ø18 × 20 mm).

which identify the elemental composition of the analyzed specimen and show distribution states of chemical elements via elemental mapping by using representative colors of each certain element, were also used to observe the dispersion and/or agglomeration of the nano-TiO_2 particles in the matrix. Small portion of specimens taken from tested cubic specimens under compressive strength test were oven-dried overnight and their SEM-EDX mapping images were captured.

Photocatalytic efficiency.

In this study, photocatalytic efficiency of the specimens was measured by using dynamic test method. According to this method, NO or both of NO and NO_2 gases flow at a constant rate and are in contact with the surface of the specimens. The gas concentration is continuously measured in real time to compare the input and output concentration of gases associated with photocatalytic degradation [52,53]. The testing parameters are summarized in Table 5.

The photocatalytic activity measurement system used in this study is schematized in Fig. 8. Photocatalytic performance was determined according to the degradation of NO gas applied to the surface of 50 × 100 × 100 mm^3 test specimens while the UV light source was on. A flow of 1000 ± 50 ppb (particle per billion) of NO gas was maintained at a rate of 3.0 l/min from a 5 mm distance, between the 50 ± 1 cm^2 specimen surface and UV permeable quartz glass. Specimens were illuminated with two Osram brand 18W UV-A blue lamps and one Philips 36W (UVA-1) white lamp. The light intensity was adjusted to 10 W/m^2 by a light intensity controller and was kept between 350 and 450 nm. NO gas, regulated in terms of flow rate and concentration, was moistened about 50–60% in the humidifying bottle before contacting the specimen surface. The NO gas used in the experiments was diluted from 100 ppm to 1 ppm using dry air. The NO gas supplied for the system at 1 bar pressure was continuously measured using the Thermo Scientific Model 42i NOx analyzer.

Since moisture content has a significant effect on photocatalytic activity [52,54,55], the specimens were dried in the oven at 45 °C for 48 h before testing to prevent moisture-related variability. After that, the specimen's relevant surface was ground, and it was placed into the reactor cabinet under UV lamps without any gas flow for 3–4 h to adapt it to the testing environment. The UV lamps were then switched off and gas flow was initiated throughout the system at the specified flow rate and concentration. At least 10 min after balancing the gas concentration passing through the system, the UV lamps were turned back on. This regulation and implementation method ensured that any measurement errors caused by the system were prevented or minimized and the testing procedure was optimized to examine NO degradation originating from the specimen. Testing was continued until NO degradation ceased,

Table 5
Photocatalytic efficiency testing parameters used in this study.

Type of Gas	NO
Gas Concentration (ppb)	1000 ± 50
Gas Flow Rate (L/min.)	3
Test Duration (min.)	30
UV Light Intensity (W/m^2)	10
Specimen Surface Area (cm^2)	50 ± 1
Analyze Method	NO degradation %

and gas flow become stable.

After completing degradation measurement, the experiment was continued until the first gas concentration was achieved by turning off the UV sources while the gas flow continued. Changes in NO and NO_2 values can be observed in the test results. NO degradation capability of the specimens was calculated by using equation given below.

$$NO_{deg}(\%) = \frac{NO_i - NO_f}{NO_i} \times 100$$

where NO_{deg}, NO_i, NO_f are degradation percentage of the NO, initial concentration of NO and final (reduced) concentration of the NO. Each test was repeated by using three different specimens and the average values were obtained.

5. Experimental results

5.1. Compressive strength

The compressive strength test results of the specimens incorporating nano-TiO_2 produced with five different mixing methods for different curing ages are shown in Table 6. The effect of mixing methods on compressive strength was evident, especially for the 1st and 2nd mixing methods. The compressive strength results of NA-3, NA-4 and NA-5 were slightly different from each other, ranging between 75.80 MPa and 78.37 MPa at the age of 28 days. As shown in the table, the highest compressive strength values at 7 and 28 days were for the NA-1: these values are 77.03 and 88.30 MPa, respectively. It can be also seen from Table 6 that the lowest strength values at 7 and 28 days were for NA-3 and NA-4. These values are 64.33 and 75.80 MPa, respectively.

Note: Numbers in parentheses are coefficients of variation (COV).

Due to the fact that the relatively smaller particle size of nano-TiO_2 provides better particle size distribution, ensuring high-density matrices and optimized particle packing of constituents because of its filler effect and flaw-bridging effect at the nano level [42,56,57], the addition of nano-TiO_2 reduced porosity and improved the microstructure of the specimens, as expected. On the other hand, nano-TiO_2 also acted as a nucleus due to the high surface areas of nano-scale materials, resulting in more nucleation sites, which provided the proper conditions for formation of hydration products. The logic behind this behavior is that small particles provide heterogeneous nucleation sites, which pull unhydrated cement particles and create more space for the formation of hydration products [58,59]. In addition, nano-scale materials have hydration agitation and acceleration effect [56–58,60]. Although it is expected, considering all these factors, that homogeneous dispersion of nano-TiO_2 in the cementitious systems prevents agglomeration problems and occurrences of weak points in the matrix and significantly increases compressive strength, this was not the case for this study. Normally, the dispersion of nanoparticles in cementitious systems can be achieved by mechanical stirring, ultrasonication, and surfactants. A combination of these techniques is reported beneficial for a homogeneous distribution of nanomaterial in cementitious matrices. The importance of dispersion of nano materials throughout the cementitious system is to reduce the required dosage for the targeted properties of cementitious system. However, compared to the literature, because of
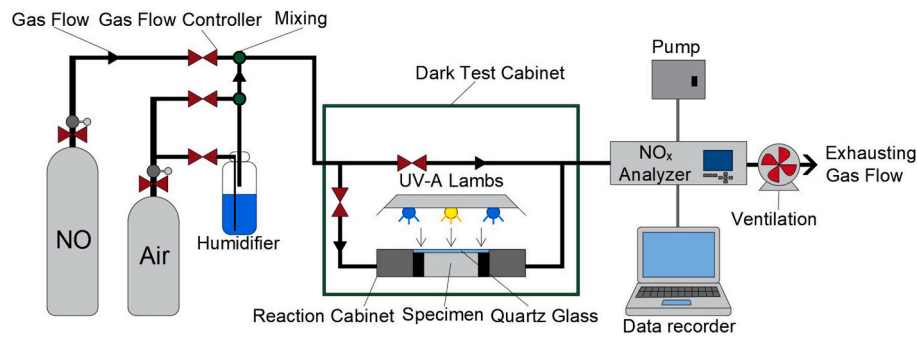
Fig. 8. Schematic view of the photocatalytic activity measurement system.

Table 6
Compressive strength, NO degradation and electrical impedance test results.

Mixture ID.	Compressive strength (MPa)		NO degradation (%)			Electrical impedance (Ω)		
	7d	28d	7d	28d	90d	7d	28d	90d
NA-1	77.03	88.30	45.2	27.4	22.4	106.7	652.8	9015.0
	(8.56)	(6.38)	(18.55)	(16.58)	(15.50)	(12.73)	(10.11)	(6.43)
NA-2	71.63	87.93	28.3	18.7	22.2	86.4	491.0	6016.0
	(4.15)	(6.03)	(12.13)	(17.95)	(15.23)	(13.41)	(6.88)	(5.54)
NA-3	64.33	78.37	32.0	21.6	23.0	166.6	1073.0	9744.0
	(5.19)	(2.13)	(20.11)	(23.10)	(19.32)	(29.06)	(20.78)	(12.14)
NA-4	65.73	75.80	40.6	39.9	30.8	67.0	250.8	3227.0
	(3.27)	(2.56)	(13.98)	(13.56)	(9.68)	(9.54)	(8.55)	(3.54)
NA-5	66.00	77.63	55.3	46.5	44.8	47.7	162.1	1864.0
	(1.00)	(1.93)	(9.88)	(7.51)	(8.19)	(11.32)	(3.08)	(3.37)

the limitation due to adequate photocatalytic activity, relatively high dosage of nano-TiO$_2$ was used (5% of total weight of binder materials) in this study. Unlike cementitious system with low dosage nano materials, ultrasonic technique has therefore limited effect on the compressive strength of cementitious systems containing high-dosage nano-TiO$_2$. In addition, the distribution of high dosage of nano particles into cement-based systems homogeneously by using ultrasonication can be quite laborious and even with relatively proper dispersion of particles, keeping them in suspended condition can require additional treatments as they tend to re-agglomerate again [39–41]. Therefore, the expected performance from nano materials may not be obtained as a satisfactory dispersion does not occur [61–63]. For the additional treatment to increase the dispersion stability and efficiency of the ultrasonication process, it was reported that utilization of different chemicals (surfactants) is needed [33,64,65] and the type, chemical content and physical properties of these surfactants are very important relating to the dispersion quality as well as the mechanical properties [65]. Therefore, the type and amount of surfactants utilized in combination with ultrasonication may require a significant optimization to ensure proper distribution of nano-particles. For NA-2 specimen in this study, the utilization of PCE (1%) as a surfactant may not have been sufficient alone to result in ultrasonication to exhibit adequate/efficient performance. For all these reasons, the strength of the systems prepared according to 1st and 2nd mixing methods were very close to each other.

As mentioned before, although it is possible to state that the better dispersion of nano materials, the higher the strength; to only evaluate nano-TiO$_2$ dispersion according to compressive strength results will, therefore, cause misleading results in the case of high dosage nano modification. When compressive strength results are evaluated, it is evident that the 1st mixing method gave the highest compressive strength at all testing ages, but a more accurate evaluation for the distribution of nano-TiO$_2$ particles throughout the matrix can be made by considering not only compressive strength but also photocatalytic performance, electrical properties and especially microstructural properties of specimens prepared with different mixing methods. To understand the relatively lower compressive strength results of NA-3 prepared with

high speed mixing, it is also important to note that this process can lead to increase in agglomeration as a result of increased ionic concentration, causing decrements in the thickness of electrical double layers [66]. As for the relatively low compressive strength performance of the NA-4 and NA-5 specimens, it can be attributed to the relatively high number of voids throughout the matrix caused by the presence of PAA [67,68]. There are many studies in the literature that show PAA utilization rate negatively affects compressive strength beyond a certain level [68–71]. Alqedra et al. [69] investigated the effects of different concentrations of PAA on the mechanical properties of concrete. The study concluded that compressive strength results of 3-day-old and 28-day-old concrete specimens increased up to a PAA utilization rate of 1%, beyond which decrements were noted. Compared to the current study, which is based on results from cement paste specimens, this limit value of 1% can be lower considering the use of concrete specimens in that study. Therefore, the compressive strength values of NA-4 and NA-5 were affected negatively by incorporation of PAA.

5.2. Electrical impedance

The electrical impedance results of the specimens incorporating nano-TiO$_2$ produced with five different mixing methods for different curing ages are shown in Table 6. Electrical impedance values increased continuously with time for all mixing methods. It is well-known that electrical conductivity of concrete is generally associated with microstructural properties [72]. Therefore, one of the most important reasons for the increase in electrical impedance values with prolonged curing time is the time-varying microstructure of the composites. Due to ongoing hydration reactions, pore structure (decrease in volume, size, and connectivity of the pores) and pore solution (decrease in ion concentration) undergo changes, and the matrix will be denser, resulting in greater electrical resistivity (and electrical impedance). Higher electrical impedance value results were observed in the first three mixing methods compared to the last two. For specimens prepared with the 1st, 2nd, and 3rd mixing methods, impedance values at 28 days varied between 491 Ω and 1073 Ω. On the other hand, the impedance values at 28

days of the NA-4 and NA-5 specimens were 250.8 Ω and 162.1 Ω, respectively. This trend was also seen for the 90-day test results: impedance values at 90 days of specimens prepared with the 1st, 2nd, and 3rd mixing methods varied between 6016 Ω and 9774 Ω, and the NA-4 and NA-5 specimens were at 3227 Ω and 1864 Ω, respectively.

As mentioned earlier, electrical conductivity of cement-based composites largely depends on their pore structure and pore solution, and the addition of nano materials has a negligible effect on the compactness, porosity, and microstructure of the matrix. On the other hand, nano-TiO_2 as a semiconductor has an enhancement effect on electrical conductivity, which could also be obtained due to the occurrence of additional conductive paths [56,73–75]. It should also be noted that both PCE and PAA have an enhancing effect on electrical conductivity

[76–78]. However, this situation was valid for all mixtures and the utilization rates of the surfactant materials in this study were low. Therefore, it is possible to state that the effect of surfactants on the electrical conductivity was too negligible to manipulate the results. It can also be stated that the electrical impedance measurements of specimens prepared with different mixing methods showed the same trend in results for each testing age, including 90 days, which is a sufficient time for almost completing the hydration process, which almost stops the change in specimen microstructure. This is, therefore, a determinative testing age for understanding the effects of the hydration process on electrical properties and observing the effects of nano-TiO_2 based on its existence and homogeneity in the matrix. Considering all these statements, comparing the results shows that the nano-TiO_2 used in the NA-5
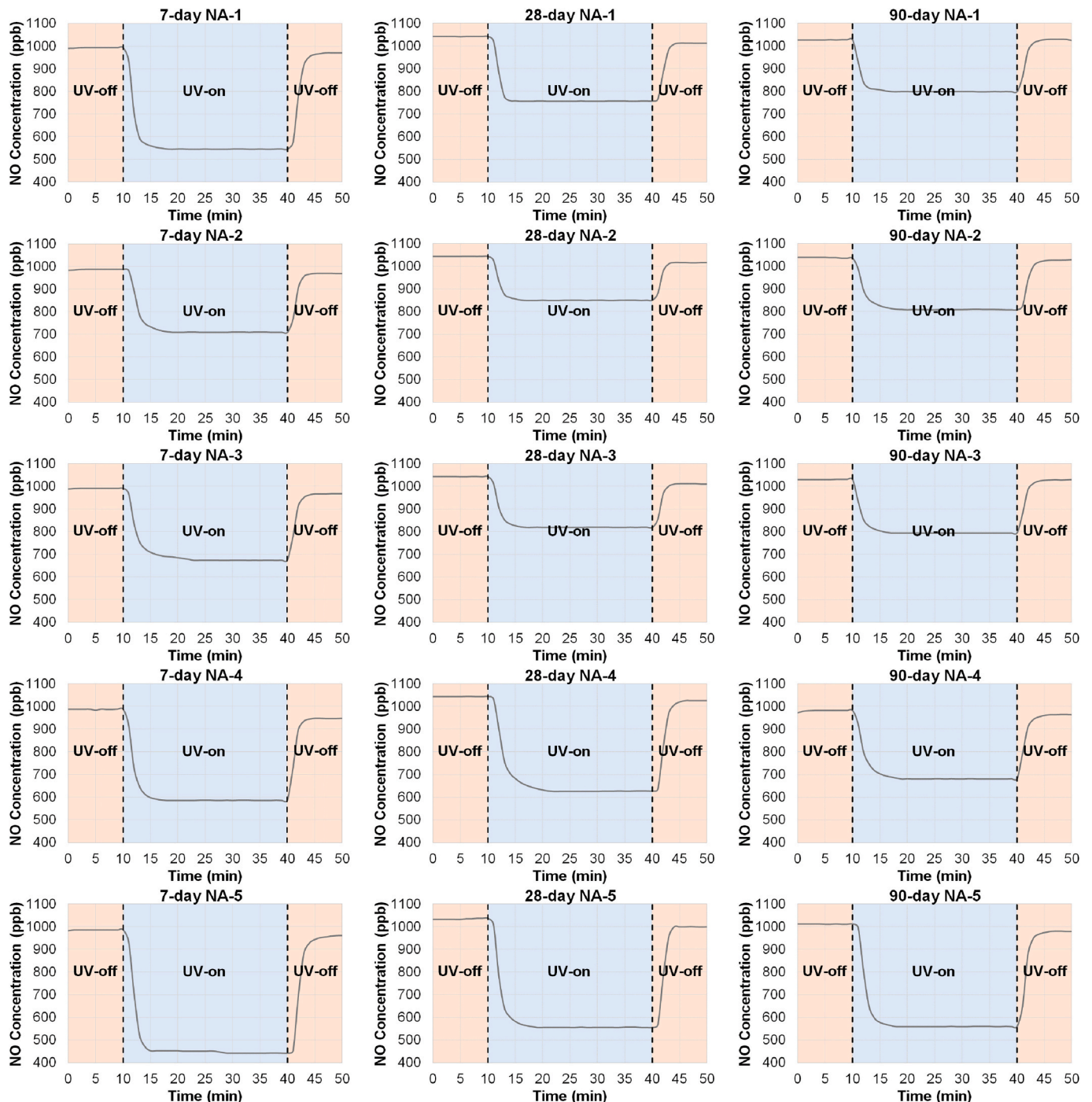

Fig. 9. Variation of NO concentration during each test.

was distributed more homogeneously, enhancing electrical conductivity due to additional conductive paths with semiconductor TiO$_2$ particles, which can be regarded as the key factor in the better electrical conductivity of specimens prepared with the 5th mixing method. The enhancing effect of incorporation of nano-TiO$_2$ on the electrical conductivity was more dominant than the electrical conductivity reducing effect due to a dense microstructure formed through the use of nano--TiO$_2$ [56]. The microstructural analysis results discussed in the next sections support these results.

5.3. Photocatalytic performance

Table 6 lists NO degradation values obtained from specimens incorporating nano-TiO$_2$, produced with five different mixing methods. Alteration graphs of the NO concentration in the reactor during each test (covering all testing periods for each test) are provided in Fig. 9. When the 7-day NO degradation results are evaluated, specimens prepared with the 5th mixing method showed a higher degradation value (55.3%) than those prepared with other methods. The 4th mixing method showed the second-highest degradation rate, which was 40.6%. The lowest degradation results for the 7-day curing age were recorded from the specimens prepared using the 2nd mixing method, with a value of
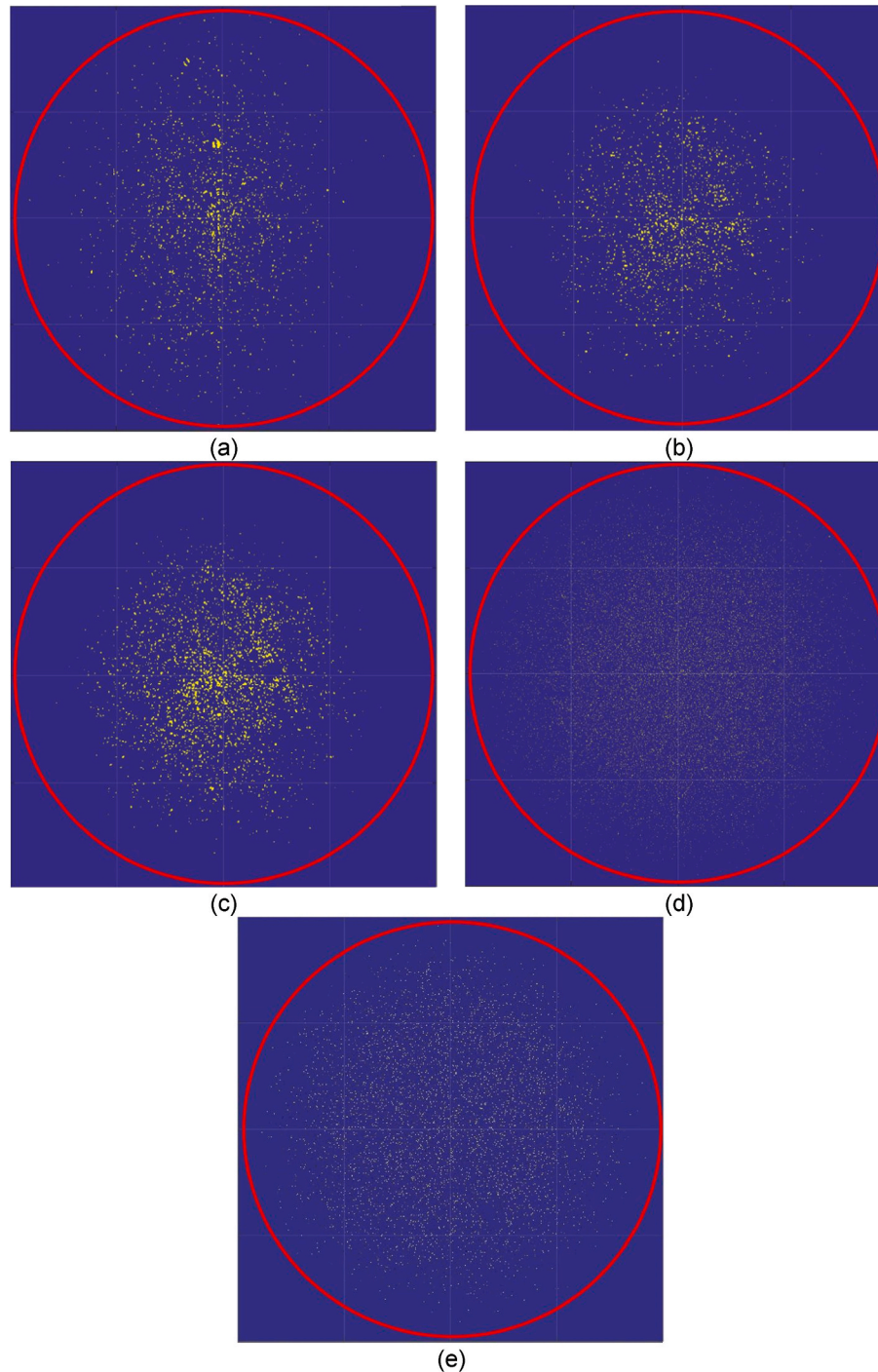

Fig. 10. CT images of the specimens prepared with different mixing methods a) NA-1, b) NA-2, c) NA-3, d) NA-4 and e) NA-5.

28.3%. The 3rd mixing method resulted in similar photocatalytic performance as the 2nd at 32.0%. It is worth noting that the photocatalytic performances of all specimens were higher at early curing ages. NO degradation results exhibited a decremental trend with further aging, most probably because TiO$_2$ particle surfaces were covered with hydration product due to ongoing hydration reactions, changing the matrix microstructure, which has also a significant effect on electrical resistivity, as mentioned before. This finding has also been reported by other researchers [79–81]. In regard to decrements in degradation results at 7- to 28- day curing ages, the highest decrement percentage was obtained from the NA-1 at 39.3%. NA-5 had the lowest decrement percentage at 19.0%. According to the 28-day NO$_x$ degradation results, the highest and lowest degradation values were again obtained from the

5th and 2nd mixing methods at 46.5% and 18.7%, respectively. At the end of the 90-day curing process, the NO degradation results of specimens prepared with the 5th mixing method was still the highest at 44.8%. NA-1, NA-2 and NA-3 showed similar photocatalytic performance with NO degradation values at 22–23%.

Table 6 and Fig. 9 show that specimens prepared with the 5th mixing method clearly exhibited significantly higher photocatalytic degradation performance. The reason for better NO degradation results in the 5th mixing method can be related to its homogeneous dispersion capability, favoring uniformity of the nano-TiO$_2$ throughout the matrix. If nano particles were not dispersed homogeneously, photocatalytic performance could be lower because of the smaller number of photocatalyst particles on UV-reached surfaces due to agglomeration problems in the
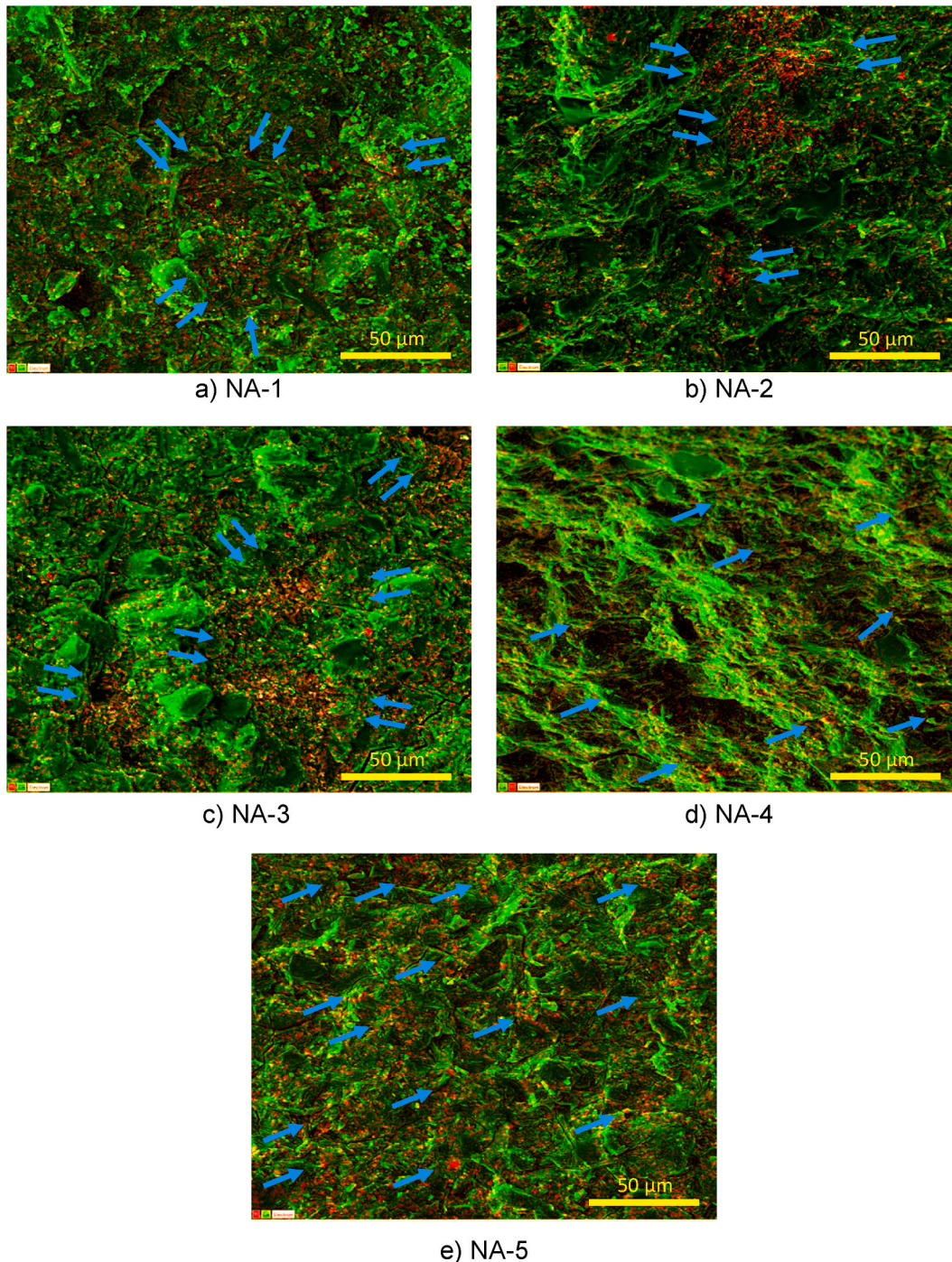

Fig. 11. SEM micrographs taken from fractured specimens at age of 90 days.

core or any point of specimens. It is also possible to state that the 5th mixing method, which resulted in uniform/homogeneous dispersion of the nano-TiO$_2$ throughout the matrix, contributed to photocatalytic performance, which is more stable and less variable over time. In terms of photocatalytic performance, it can be also concluded that in NA-4 and NA-5, the effect of PAA on nano-TiO$_2$ dispersion was significantly evident.

5.4. Microstructural characteristics

As for the microstructure of the specimens, cross-section views obtained by the computed tomography device are shown in Fig. 10: the yellow dots indicate TiO$_2$ particles. Fig. 10-d and 10-e show that the nano-TiO$_2$ particles have been well-dispersed and there is no sign of agglomeration throughout the cross-section of the matrix. Therefore, the stable photocatalytic performances of these specimens can be attributed to proper distribution of the nano-TiO$_2$ particles, in the case of the 4th and 5th mixing methods. The highest NO degradation result of NA-5 was also related with proper dispersion of the nano-TiO$_2$ particles, which ensured the presence of relatively high-TiO$_2$ particles on the specimen surface reached by UV light. On the other hand, NA-3 has been shown to have lower photocatalytic performance due to agglomeration problems related to nano-sized TiO$_2$, resulting in instability throughout the matrix that can be seen in Fig. 10-c. Due to the agglomeration problem associated with the surface charge of particles resulting nonhomogeneous dispersion, the vast majority of particles can remain at depths that prevent them from coming into contact with UV light. This is, therefore, a situation that prevents further photocatalytic reaction. Although this is also valid for the 1st and 2nd mixing methods, it is more evident for the 3rd method, which can be easily seen from Fig. 10.

SEM/EDX results.

The dispersion of Ti elements in the mixtures prepared with different mixing methods is demonstrated in Fig. 11. SEM/EDX mapping micrographs show that the dispersion of Ti elements was quite different between specimens. It is clear that the Ti particles (indicated in red) are distributed very homogeneously in the cross-section of NA-5 (Fig. 11-e), which is also evidence of the good nano-TiO$_2$ dispersion capability of the 5th mixing method. The significantly better NO degradation capability and higher electrical conductivity performance of NA-4 and NA-5 compared to the others allows us to conclude that PAA considerably contributes to homogeneous distribution of nano-sized TiO$_2$ particles throughout the matrix. It has been reported that the fluidity of specimens can affect their homogeneity [82]. It is therefore very likely that the higher fluidity of NA-5 (along with the presence of PAA) leads to relatively more homogeneous systems, further improving the microstructural properties of mixtures in favor of photocatalytic efficiency. As for the NA-3 specimen, it can be easily observed from Fig. 11-c that the 3rd mixing method caused high-level agglomeration. Fig. 11-a and 11-b show some agglomeration zones throughout NA-1 and NA-2.

6. Discussions

6.1. Influence of the mixing method on compressive strength of cementitious composites

Compressive strength tests showed an incremental trend for all mixtures, regardless of mixing methods, which can be attributed to ongoing hydration and further curing. Increments were more pronounced in NA-2 and NA-3 than in NA-1, NA-4 and NA-5. The increment rates in the compressive strength results of NA-1, NA-2, NA-3, NA-4, NA-5 specimens from 7 to 28 days were 14.6% (from 77.03 to 88.30 MPa), 22.76% (from 71.63 to 87.93 MPa), 21.82% (from 64.33 to 78.37 MPa), 15.32% (from 65.73 to 75.80 MPa) and 17.62% (from 66.00 to 77.63 MPa), respectively. When the COV (the ratio of the standard deviation of a number of measurements to the arithmetic mean) values in Table 6 are evaluated, the COV values of NA-5 were 1.0% and 1.93% for 7 days and

28 days curing age, respectively, the lowest ones for each age. Although the compressive strength results of NA-1 were the highest for all curing ages, the individual strength values of six different replicates varied significantly, with COV values of 8.56% for 7 days and 6.38% for 28 days as the highest ones. COV values of NA-2, NA-3 and N-4 were 4.15%, 5.19% and 3.27% for 7 days and 6.03%, 2.13% and 2.26% for 28 days respectively, which were higher than NA-5 results and lower than NA-1. Relatively low COV values of NA-5 specimens indicate that individual strength values of these specimens were concordant with each other, showing consistent results throughout the test. This low variability between the results can be attributed to the capability of the 5th mixing method to distribute nano particles homogeneously throughout the matrix. Consequently, homogeneously incorporating nano-sized TiO$_2$ particles into the matrix with a proper mixing process is believed to provide a stable and uniform microstructure and thereby obtaining reproducible products with more consistent performance.

6.2. Influence of the mixing method on NO degradation of cementitious composites

In mixtures containing nano-TiO$_2$ particles, the highest photocatalytic efficiency was obtained by using the 5th mixing methods, regardless of curing age. NO degradation rates were the most stable with prolonged curing ages compared to other mixtures. Degradation values at 7, 28 and 90 days were 55.3%, 46.5% and 44.8%, respectively. In terms of COV values related with NO degradation capability of the specimens given in Table 6, the NO degradation results of NA-5 replicates have shown least variation as with other test methods used in this study. Several previous studies have measured photocatalytic efficiency of cement-based composites containing different types of photocatalysts with different properties arising from their production process and differing ingredients. However, many of those studies used standards related to measurement of photocatalytic efficiency that have since been revised. There are also many differences between the ingredients used in different studies. Therefore, it is not possible to make a direct comparison. Nonetheless, it is possible to look at those that used mixtures with minimum common characteristics with those of current study. Hüsken et al. [14] investigated the effects of different parameters related to the production process. When they compared degradation rate results, they observed that pretreatment on surfaces where photocatalytic reactions occur (surface conditions), the technique used to incorporate TiO$_2$ into the composition (application technique), as well as the applied light source and pigments used for aesthetic concerns all have major influences on NO degradation capability. Their degradation rate results, in accordance with product-related parameters, ranged from 2.9 to 39.6%. All NO degradation results of NA-5 in the current study are significantly higher than those of the study conducted by Husken et al. [14]. For the specimen in their study, which has almost the same parameters as NA-5 (such as 5% TiO$_2$ content and incorporation of TiO$_2$ with a prepared suspension), the degradation value was 16.5%, which is significantly lower than that of NA-5. In another research study from the same authors [83], they reported a 30% degradation rate for the specimen containing 5% TiO$_2$. According to Ballari et al. [84], 100 × 200 mm specimens (about twice the area of those used in the current study) were used and the maximum NO degradation value of specimens under almost the same conditions as NA-5 was 43.3%. Although its surface was wider than that of NA-5 and its TiO$_2$ content was 5.9%, their specimen showed almost the same photocatalytic efficiency performance as NA-5. Considering these comparisons, it can be stated that the incorporation technique of nano materials, additives and additional ingredients used for homogenous distribution have an undeniable influence on specific performances of the final product, including photocatalytic efficiency. In this study, developing only the mixing method undeniably improved the mixture properties. One of the main goals was to investigate the effect of mixing procedure or technique on photocatalytic performance, and it has confirmed that the NO degradation capability of NA-5 can be

improved by implementing different processes and parameters around measuring procedures, measurement process related parameters, and some product-related parameters or processes. For example, according to Hüsken et al. [14], using the sand blasting process on the UV-reachable surface before NO degradation rates are measured significantly increases NO degradation capability compared to the grinding process, which was also used in the current study. Therefore, as mentioned above, the photocatalytic efficiency of NA-5 (which was the best one for the current study) can be advanced by different improvement techniques.

6.3. Influence of the mixing method on electrical impedance of cementitious composites

To determine electrical conductivity performance, three different parts of the same specimen were used to monitor the conductivity behavior of the whole cast specimen (as mentioned earlier). The results obtained from different parts of two identical specimens for each mixing method is a more realistic parameter for revealing the overall microstructure of the matrix in terms of homogeneity and homogenous dispersion of semi-conductive nano-TiO_2 particles. In this study, individual EI results of six NA-5 replicates for late age were closest to each other, possessing very small COV values of 3.08% for 28-days and 3.37 for 90-day curing ages, compared to specimens prepared with other mixing methods. The low variability between EI results from the 5th mixing method was expected, considering microstructural properties and NO degradation capability of NA-5. Thereby, it can be definitively stated that the variability between results found in this study reveals the effect of the mixing process on matrix microstructure. Additionally, considering that the COV value of the NA-4 at the 90-day curing age was relatively low compared to the others, therefore use of PAA has undeniable benefits for obtaining more reliable and uniform EI results due to the homogeneous microstructure of specimens. The highest COV values of EI results of NA-3 replicates for all curing ages have also proven that high-speed mixing leads to agglomeration problems, as mentioned in Section 5.1. The COV values were in line with the other test methods used in this study as ranking especially with those of NO degradation test. However, the COV values of NO degradation results were arithmetically greater than those of EI test.

Based on the abovementioned statements, the EI test is a more effective method for evaluating homogeneous distribution of conductive nanoparticles throughout the matrix. On the other hand, variable EI test results for all matrix specimens showed a decreasing trend with prolonged curing age, regardless of mixing method. It should be noted that the effect of porosity, pore solution chemistry and tortuosity of the pore network on electrical conductivity is more pronounced, especially at early ages, due to the uncompleted hydration process. These are the main parameters influencing electrical conductivity of cement-based composites [72]. Therefore, the pore structure of every replicate specimen prepared with different mixing methods is quite different at early age. Pores are gradually closed by ongoing hydration, and the majority of the pore solution is consumed by the ongoing hydration process. In addition, paths between pores disappear as they are covered by hydration products. Due to the effect of final hydration products on pore characteristics, the manipulative characteristics of these parameters in terms of EI values are eliminated at late curing ages. Consequently, the decremental trend in variability between EI results with prolonged curing age may be due to the occurrence of more stable and regular microstructure at the end of the hydration process. A similar trend was also observed for the correlation between NO degradation and EI test results. This correlation, directly associated with the presence of semi-conductive nano-TiO_2 particles and their homogeneous distribution throughout the matrix, tended to get stronger with prolonged curing age (Fig. 12). At the end of 90-day curing, the correlation was strong, with a coefficient of correlation value of 0.89. Based on the above-mentioned explanations and Fig. 12, it is possible to state that there is a significant relationship between electrical conductivity and photocatalytic efficiency regardless of mixing method, although this relationship becomes more evident with prolonged curing time.

One of the main aims of this study was to obtain reliable, reproducible products with the same performances associated with microstructural property. This can be ensured by homogeneous and uniform distribution of ingredients throughout the matrix. As mentioned before, the electrical property and NO degradation capability of cement-based composites are strongly associated with their microstructural properties. EI results and NO degradation rates both changed depending on curing age. This variation can be attributed to the changed microstructure of cement-based composites with prolonged curing ages. For the cement-based composites containing TiO_2 as a photocatalyst, the dispersion of semi-conductive TiO_2 throughout the entire volume of the specimens (which can be considered as the path of the electric current) is the main criteria for increasing electrical conductivity. On the other hand, NO degradation capability or photocatalytic efficiency depends on the presence and amount of TiO_2 in the UV-accessible surface of the
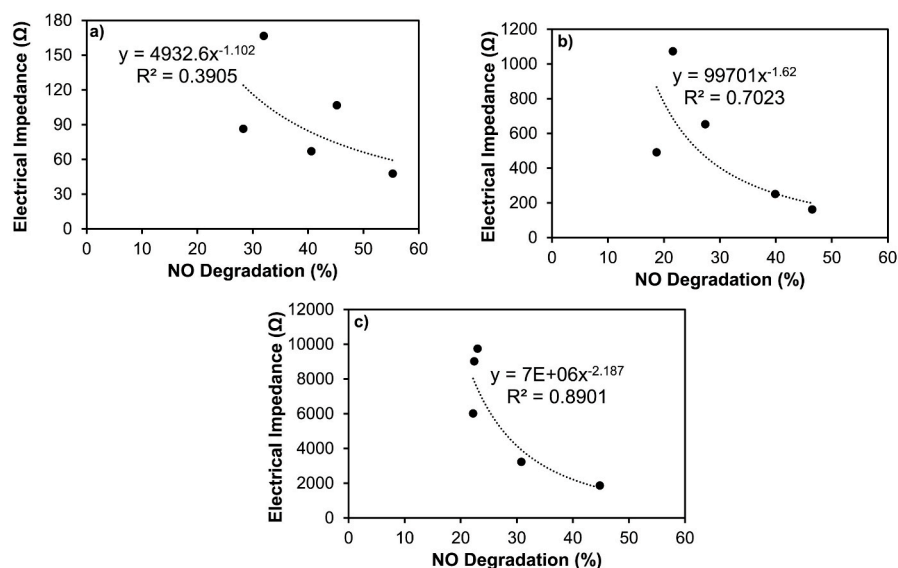

Fig. 12. Electrical impedance versus NO degradation results of each specimen for a) 7 days b) 28 days c) 90 days.

specimen rather than its entire volume. To stimulate photocatalytic reactions and ensure satisfying photocatalytic efficiency, it is necessary to ensure there are sufficient photocatalysts on the surfaces where UV light can reach. Agglomeration of nano-TiO_2 on the surface where the photocatalytic reactions occur can contribute to the NO degradation capability of cement-based composites, but this type of agglomeration cannot be guaranteed. Therefore, the purpose of the uniform dispersion of nano-TiO_2 particles was to increase of number of TiO_2 particles distributed throughout the matrices as much as possible to obtain reliable reproducible products with the same performance. Homogeneous dispersion of nanoparticles in the mixtures eliminates embedded particles that remain lumpy in the dark depths of composites due to the agglomeration effects of nanoparticles and increases/guarantees the presence of photocatalyst particles on the specimen's surface illuminated by UV light. In a general sense, it is possible to state that factors associated with microstructural properties of cement-based composites influencing EI results are also generally effective on NO degradation results. However, NO degradation capability can be more easily affected because of its dependence on the conditions of a single surface, and accordingly, the possibility of surrounding the TiO_2 particles too close to the surface or on the surface with ongoing hydration products.

7. Conclusions

The purpose of this study is to investigate the effects of different mixing techniques and surfactant materials on the dispersion of high dosage nano-TiO_2 throughout cement-based materials. Five different mixing methods based on three mixing techniques: ultrasonication, hand blender and conventional cement mixer, as well as two surfactant materials: polycarboxylate based superplasticizer (PCE) and polyacrylic acid (PAA) were used. All specimens created with these methods were evaluated in terms of nano-TiO_2 dispersion throughout the cement-based mixtures. The main aim was to ensure good dispersion of the nano-TiO_2 in the matrix to maximize NO degradation capability of the mixtures by using a large part of the nano-TiO_2 incorporated into the mixtures for photocatalytic activity. To evaluate dispersion, electrical impedance and compressive strength values were measured, photocatalytic performance of the specimens was determined, and microstructural analysis was performed. Conclusions are as follows:

- The amplitude of the ultrasonication process was highly influential on zeta potential, which increased negatively with increasing amplitude value applied. The effect of using surfactant materials on the zeta potential was also evident. The zeta potential of the suspension increased negatively to a certain level with increased utilization rates of surfactant materials.
- Use of PAA resulted in higher electrical conductivity due to the occurrence of additional conductive paths and owing to the better dispersion of semi-conductive nano-TiO_2 materials.
- Irrespective of the test, the results obtained from specimens with higher NO degradation capability were largely concordant with each other. Therefore, uniform dispersion of nano-scale materials throughout cement-based matrix provides stable and uniform microstructure, and these specimens can be considered a reliable, reproducible products with the same performance.
- Photocatalytic performances of the specimens decreased with time. The specimens prepared more homogenously showed the highest NO degradation rates. The degradation capability of these specimens was more stable with prolonged curing ages.
- The correlation between NO degradation rates and EI results is directly associated with the presence of semi-conductive nano-TiO_2 particles and their homogeneous distribution throughout the matrix, which tended to get stronger with prolonged curing age. Regardless of mixing method, there is a significant relationship between electrical conductivity and photocatalytic efficiency, which becomes more evident with prolonged curing time. Therefore, electrical

properties of composites containing photocatalytic semi-conductive materials can provide a reliable estimate of the photocatalytic efficiency of them.
- In the presence of PAA, greater fluidity resulted from including PCE leads in relatively more homogeneous systems, providing mixtures with the ability to further improve their microstructural properties in favor of photocatalytic efficiency. Therefore, greater fluidity can contribute to homogeneous dispersion of ingredients throughout the matrix.
- Finally, the results indicate that the 5th mixing method has a higher capability to evenly disperse high dosage TiO_2 materials at the nanoscale, without sacrificing any other properties. The effect of PAA was more pronounced for better dispersion of the nano-TiO_2 in the matrix. Incorporating nano-TiO_2 into cement-based mixtures using the ultrasonication process and binary utilization of PCE and PAA can provide better dispersion of the nano-scale particles throughout the matrix.

Declaration of competing interest

The authors declare that they have no known competing financial interests or personal relationships that could have appeared to influence the work reported in this paper.

Acknowledgement

References

[1] D. Tristantini, R. Mustikasari, Modification of TiO_2 nanoparticle with PEG and SiO_2 for anti-fogging and self-cleaning application, Int. J. Eng. Technol. 11 (2) (2011) 80–85.

[2] D.M. Chien, N.N. Viet, N.T.K. Van, N.T.P. Phong, Characteristics modification of TiO2 thin films by doping with silica and alumina for self-cleaning application, J. Exp. Nanosci. 4 (3) (2009) 221–232, https://doi.org/10.1080/17458080902920506.

[3] T.K. Tseng, Y.S. Lin, Y.J. Chen, H. Chu, A review of photocatalysts prepared by sol-gel method for VOCs removal, Int. J. Mol. Sci. 11 (6) (2010) 2336–2361, https://doi.org/10.3390/ijms11062336.

[4] Q. Zhang, J.-B. Joo, Z. Lu, M. Dahl, D.Q.L. Oliveira, M. Ye, Y. Yin, Self-assembly and photocatalysis of mesoporous TiO_2 nanocrystal clusters, Nano Res 4 (1) (2011) 103–114, https://doi.org/10.1007/s12274-010-0058-9.

[5] S. Anandan, T. Narasinga Rao, M. Sathish, D. Rangappa, I. Honma, M. Miyauchi, Superhydrophilic graphene-loaded TiO2 thin film for self-cleaning applications, ACS Appl. Mater. Interfaces 5 (1) (2013) 207–212, https://doi.org/10.1021/am302557z.

[6] B.-M. Kim, H.M. Yadav, J.-S. Kim, Self-cleaning performance of sol–gel-derived TiO_2/SiO_2 double-layer thin films, J. Coating Technol. Res. 13 (5) (2016) 905–910, https://doi.org/10.1007/s11998-016-9804-6.

[7] H.E. Çamurlu, Ö. Kesmez, E. Burunkaya, N. Kiraz, Z. Yeşil, M. Asiltürk, E. Arpaç, Sol-gel thin films with anti-reflective and self-cleaning properties,, Chem. Pap. 66 (5) (2012) 461–471, https://doi.org/10.2478/s11696-012-0144-4.

[8] Z. Yuan, B. Li, J. Zhang, C. Xu, J. Ke, Synthesis of TiO_2 thin film by a modified sol-gel method and properties of the prepared films for photocatalyst, J. Sol. Gel Sci. Technol. 39 (3) (2006) 249–253, https://doi.org/10.1007/s10971-006-8164-6.

[9] O. Carp, C.L. Huisman, A. Reller, Photoinduced reactivity of titanium dioxide, Prog. Solid State Chem. 32 (1–2) (2004) 33–177, https://doi.org/10.1016/j.progsolidstchem.2004.08.001.

[10] V.r. Zivica, A. Bajza, Acidic attack of cement based materials—a review.: Part 1. Principle of acidic attack, Construct. Build. Mater. 15 (8) (2001) 331–340, https://doi.org/10.1016/S0950-0618(01)00012-5.

[11] H. Chen, A. Namdeo, M. Bell, Classification of road traffic and roadside pollution concentrations for assessment of personal exposure, Environ. Model. Software 23 (3) (2008) 282–287, https://doi.org/10.1016/j.envsoft.2007.04.006.

[12] J. Zhao, X. Yang, Photocatalytic oxidation for indoor air purification: a literature review, Build. Environ. 38 (5) (2003) 645–654, https://doi.org/10.1016/S0360-1323(02)00212-3.

[13] S. Hager, R. Bauer, G. Kudielka, Photocatalytic oxidation of gaseous chlorinated organics over titanium dioxide, Chemosphere 41 (8) (2000) 1219–1225, https://doi.org/10.1016/S0045-6535(99)00558-5.

[14] G. Hüsken, M. Hunger, H. Brouwers, Experimental study of photocatalytic concrete products for air purification, Build. Environ. 44 (12) (2009) 2463–2474, https://doi.org/10.1016/j.buildenv.2009.04.010.

[15] S. Wang, H.M. Ang, M.O. Tade, Volatile organic compounds in indoor environment and photocatalytic oxidation: state of the art, Environ. Int. 33 (5) (2007) 694–705, https://doi.org/10.1016/j.envint.2007.02.011.

[16] L. Znaidi, R. Seraphimova, J.F. Bocquet, C. Colbeau-Justin, C. Pommier, A semi-continuous process for the synthesis of nanosize TiO2 powders and their use as photocatalysts, Mater. Res. Bull. 36 (5–6) (2001) 811–825, https://doi.org/10.1016/S0025-5408(00)00482-7.

[17] M. Anpo, T. Shima, S. Kodama, Y. Kubokawa, Photocatalytic hydrogenation of propyne with water on small-particle titania: size quantization effects and reaction intermediates, J. Phys. Chem. 91 (16) (1987) 4305–4310.

[18] L. Cao, A. Huang, F.-J. Spiess, S.L. Suib, Gas-phase oxidation of 1-butene using nanoscale TiO2 photocatalysts, J. Catal. 188 (1) (1999) 48–57, https://doi.org/10.1006/jcat.1999.2596.

[19] L. Cao, Z. Gao, S.L. Suib, T.N. Obee, S.O. Hay, J.D. Freihaut, Photocatalytic oxidation of toluene on nanoscale TiO2 catalysts: studies of deactivation and regeneration, J. Catal. 196 (2) (2000) 253–261, https://doi.org/10.1006/jcat.2000.3050.

[20] L. Gao, Q. Zhang, Effects of amorphous contents and particle size on the photocatalytic properties of TiO2 nanoparticles, Scripta Mater. 44 (8–9) (2001) 1195–1198, https://doi.org/10.1016/S1359-6462(01)00681-9.

[21] Y. Ohama, D. Van Gemert, Application of Titanium Dioxide Photocatalysis to Construction Materials: State-Of-The-Art Report of the RILEM Technical Committee 194-TDP, Springer Science & Business Media, 2011.

[22] H. He, C. Liu, K.D. Dubois, T. Jin, M.E. Louis, G. Li, Enhanced charge separation in nanostructured TiO2 materials for photocatalytic and photovoltaic applications, Ind. Eng. Chem. Res. 51 (37) (2012) 11841–11849, https://doi.org/10.1021/ie300510n.

[23] S. Kawashima, J.-W.T. Seo, D. Corr, M.C. Hersam, S.P. Shah, Dispersion of CaCO3 nanoparticles by sonication and surfactant treatment for application in fly ash–cement systems, Mater. Struct. 47 (6) (2014) 1011–1023, https://doi.org/10.1617/s11527-013-0110-9.

[24] B.M. Tyson, R.K.A. Al-Rub, A. Yazdanbakhsh, Z. Grasley, A quantitative method for analyzing the dispersion and agglomeration of nano-particles in composite materials, Compos. B Eng. 42 (6) (2011) 1395–1403, https://doi.org/10.1016/j.compositesb.2011.05.020.

[25] A. Yazdanbakhsh, Z. Grasley, B. Tyson, R.K.A. Al-Rub, Dispersion quantification of inclusions in composites, Compos. Appl. Sci. Manuf. 42 (1) (2011) 75–83, https://doi.org/10.1016/j.compositesa.2010.10.005.

[26] A. Sobolkina, V. Mechtcherine, V. Khavrus, D. Maier, M. Mende, M. Ritschel, A. Leonhardt, Dispersion of carbon nanotubes and its influence on the mechanical properties of the cement matrix, Cement Concr. Compos. 34 (10) (2012) 1104–1113, https://doi.org/10.1016/j.cemconcomp.2012.07.008.

[27] N. Lakshminarasimhan, W. Kim, W. Choi, Effect of the agglomerated state on the photocatalytic hydrogen production with in situ agglomeration of colloidal TiO2 nanoparticles, J. Phys. Chem. C 112 (51) (2008) 20451–20457, https://doi.org/10.1021/jp808541v.

[28] A. Folli, I. Pochard, A. Nonat, U.H. Jakobsen, A.M. Shepherd, D.E. Macphee, Engineering photocatalytic cements: understanding TiO2 surface chemistry to control and modulate photocatalytic performances, J. Am. Ceram. Soc. 93 (10) (2010) 3360–3369, https://doi.org/10.1111/j.1551-2916.2010.03838.x.

[29] A. Folli, U. Jakobsen, G. Guerrini, D. Macphee, Rhodamine B discolouration on TiO2 in the cement environment: a look at fundamental aspects of the self-cleaning effect in concretes, J. Adv. Oxid. Technol. 12 (1) (2009) 126–133, https://doi.org/10.1515/jaots-2009-0116.

[30] K. Sato, J.G. Li, H. Kamiya, T. Ishigaki, Ultrasonic dispersion of TiO2 nanoparticles in aqueous suspension, J. Am. Ceram. Soc. 91 (8) (2008) 2481–2487, https://doi.org/10.1111/j.1551-2916.2008.02493.x.

[31] S.H. Othman, S. Abdul Rashid, T.I. Mohd Ghazi, N. Abdullah, Dispersion and stabilization of photocatalytic TiO2 nanoparticles in aqueous suspension for coatings applications, J. Nanomater. 2012 (2012) 1687–4110, https://doi.org/10.1155/2012/718214.

[32] A. Yousefi, A. Allahverdi, P. Hejazi, Effective dispersion of nano-TiO2 powder for enhancement of photocatalytic properties in cement mixes, Construct. Build. Mater. 41 (2013) 224–230, https://doi.org/10.1016/j.conbuildmat.2012.11.057.

[33] O. Mendoza, G. Sierra, J.I. Tobón, Influence of super plasticizer and Ca(OH)2 on the stability of functionalized multi-walled carbon nanotubes dispersions for cement composites applications, Construct. Build. Mater. 47 (2013) 771–778, https://doi.org/10.1016/j.conbuildmat.2013.05.100.

[34] S. Alrekabi, A. Cundy, A. Lampropoulos, I. Savina, Experimental investigation on the effect of ultrasonication on dispersion and mechanical performance of multi-wall carbon nanotube-cement mortar composites, Int. J. Civ. Environ. Eng. 10 (3) (2016) 261–267, https://doi.org/10.5281/zenodo.1112027.

[35] M. Saafi, K. Andrew, P.L. Tang, D. McGhon, S. Taylor, M. Rahman, S. Yang, X. Zhou, Multifunctional properties of carbon nanotube/fly ash geopolymeric nanocomposites, Construct. Build. Mater. 49 (2013) 46–55, https://doi.org/10.1016/j.conbuildmat.2013.08.007.

[36] N. Yazdani, V. Mohanam, Carbon nano-tube and nano-fiber in cement mortar: effect of dosage rate and water-cement ratio, Int. J. Mater. Sci. 4 (2) (2014) 45–52, https://doi.org/10.14355/ijmsci.2014.0402.01.

[37] M.-H. Zhang, J. Islam, S. Peethamparan, Use of nano-silica to increase early strength and reduce setting time of concretes with high volumes of slag, Cement Concr. Compos. 34 (5) (2012) 650–662, https://doi.org/10.1016/j.cemconcomp.2012.02.005.

[38] M.-H. Zhang, J. Islam, Use of nano-silica to reduce setting time and increase early strength of concretes with high volumes of fly ash or slag, Construct. Build. Mater. 29 (2012) 573–580, https://doi.org/10.1016/j.conbuildmat.2011.11.013.

[39] S.J. Chen, C.Y. Qiu, A.H. Korayem, M.R. Barati, W.H. Duan, Agglomeration process of surfactant-dispersed carbon nanotubes in unstable dispersion: a two-stage agglomeration model and experimental evidence, Powder Technol. 301 (2016) 412–420, https://doi.org/10.1016/j.powtec.2016.06.033.

[40] G.H. Kirby, J.A. Lewis, Comb polymer architecture effects on the rheological property evolution of concentrated cement suspensions, J. Am. Ceram. Soc. 87 (9) (2004) 1643–1652, https://doi.org/10.1111/j.1551-2916.2004.01643.x.

[41] P. Sikora, A. Augustyniak, K. Cendrowski, P. Nawrotek, E. Mijowska, Antimicrobial activity of Al2O3, CuO, Fe3O4, and ZnO nanoparticles in scope of their further application in cement-based building materials, Nanomaterials 8 (4) (2018) 212, https://doi.org/10.3390/nano8040212.

[42] A. Al-Dahawi, O. Öztürk, F. Emami, G. Yıldırım, M. Şahmaran, Effect of mixing methods on the electrical properties of cementitious composites incorporating different carbon-based materials, Construct. Build. Mater. 104 (2016) 160–168, https://doi.org/10.1016/j.conbuildmat.2015.12.072.

[43] Cement CEN, Part 1: Composition, Specifications and Conformity Criteria for Common Cements, European Committee for Standardization Brussels, 2011.

[44] M.M. Ba-Abbad, A.A.H. Kadhum, A.B. Mohamad, M.S. Takriff, K. Sopian, Synthesis and catalytic activity of TiO2 nanoparticles for photochemical oxidation of concentrated chlorophenols under direct solar radiation, Int. J. Electrochem. Sci. 7 (6) (2012) 4871–4888.

[45] T. Theivasanthi, M. Alagar, Titanium dioxide (TiO2) nanoparticles XRD analyses: an insight, Chem. Phys. (2013). https://arxiv.org/abs/1307.1091.

[46] ASTM C494/C494M—15a, Standard Specification for Chemical Admixtures for Concrete, 2011.

[47] S. Fazio, J. Guzman, M. Colomer, A. Salomoni, R. Moreno, Colloidal stability of nanosized titania aqueous suspensions, J. Eur. Ceram. Soc. 28 (11) (2008) 2171–2176, https://doi.org/10.1016/j.jeurceramsoc.2008.02.017.

[48] S. Musso, J.-M. Tulliani, G. Ferro, A. Tagliaferro, Influence of carbon nanotubes structure on the mechanical behavior of cement composites, Compos. Sci. Technol. 69 (11–12) (2009) 1985–1990, https://doi.org/10.1016/j.compscitech.2009.05.002.

[49] V.C. Moore, M.S. Strano, E.H. Haroz, R.H. Hauge, R.E. Smalley, J. Schmidt, Y. Talmon, Individually suspended single-walled carbon nanotubes in various surfactants, Nano Lett. 3 (10) (2003) 1379–1382, https://doi.org/10.1021/nl034524j.

[50] A. S. T. M, ASTM C109-Standard Test Method for Compressive Strength of Hydraulic Cement Mortars, ASTM International, West Conshohocken, PA, 2008.

[51] T.-C. Hou, Wireless and Electromechanical Approaches for Strain Sensing and Crack Detection in Fiber Reinforced Cementitious Materials, PhD Thesis, 2008.

[52] P. Baglioni, L. Cassar, K. Hashimoto, F. Filippone, G. Mattioli, A.A. Bonapasta, C. L. Bianchi, S. Ardizzone, G. Cappelletti, C. Pirola, International RILEM Symposium on Photocatalysis, Environment and Construction Materials-TDP 2007, RILEM Publications, Bagneux, France, 2007, pp. 171–177.

[53] A.R. Jayapalan, B.Y. Lee, E.M. Land, M.H. Bergin, K.E. Kurtis, Photocatalytic efficiency of cement-based materials: demonstration of proposed test method, ACI Mater. J. 112 (2) (2015) 219, https://doi.org/10.14359/51686985.

[54] H. Dylla, M.M. Hassan, L.N. Mohammad, T. Rupnow, E. Wright, Evaluation of environmental effectiveness of titanium dioxide photocatalyst coating for concrete pavement, Transport. Res. Rec. 2164 (1) (2010) 46–51, https://doi.org/10.3141/2164-06.

[55] D. Seo, T.S. Yun, NOx removal rate of photocatalytic cementitious materials with TiO2 in wet condition, Build, Environ. Times 112 (2017) 233–240, https://doi.org/10.1016/j.buildenv.2016.11.037.

[56] Z. Li, B. Han, X. Yu, S. Dong, L. Zhang, X. Dong, J. Ou, Effect of nano-titanium dioxide on mechanical and electrical properties and microstructure of reactive powder concrete, Mater. Res. Express 4 (9) (2017), 095008, https://doi.org/10.1088/2053-1591/aa87db.

[57] E. Mohseni, B.M. Miyandehi, J. Yang, M.A. Yazdi, Single and combined effects of nano-SiO2, nano-Al2O3 and nano-TiO2 on the mechanical, rheological and durability properties of self-compacting mortar containing fly ash, Construct. Build. Mater. 84 (2015) 331–340, https://doi.org/10.1016/j.conbuildmat.2015.03.006.

[58] J. Chen, S.-c. Kou, C.-s. Poon, Hydration and properties of nano-TiO2 blended cement composites, Cem. Concr.ete Compos. 34 (5) (2012) 642–649, https://doi.org/10.1016/j.cemconcomp.2012.02.009.

[59] X. Wang, K. Wang, J. Tanesi, A. Ardani, Effects of nanomaterials on the hydration kinetics and rheology of portland cement pastes, Adv. Civ. Eng. Mater. 3 (2) (2014) 142–159, https://doi.org/10.1520/ACEM20140021.

[60] B. Han, L. Zhang, S. Zeng, S. Dong, X. Yu, R. Yang, J. Ou, Nano-core effect in nano-engineered cementitious composites, Compos. Appl. Sci. Manuf. 95 (2017) 100–109, https://doi.org/10.1016/j.compositesa.2017.01.008.

[61] S. Alrekabi, A. Cundy, R.L.D. Whitby, A. Lampropoulos, I. Savina, Effect of undensified silica fume on the dispersion of carbon nanotubes within a cementitious composite, J. Phys.: Conf. Series 829 (2017), 012011, https://doi.org/10.1088/1742-6596/755/1/011001.

[62] R. Mateos, S. Vera, M. Valiente, M.D. Díez-Pascual, M.P. San Andrés, Comparison of anionic, cationic and nonionic surfactants as dispersing agents for graphene based on the fluorescence of riboflavin, Nanomaterials 7 (11) (2017) 403, https://doi.org/10.3390/nano7110403.

[63] O. Mendoza, G. Sierra, J.I. Tobón, Effect of the reagglomeration process of multi-walled carbon nanotubes dispersions on the early activity of nanosilica in cement composites, Construct. Build. Mater. 54 (2014) 550–557, https://doi.org/10.1016/j.conbuildmat.2013.12.084.

[64] S. Chen, F.G. Collins, A.J.N. MacLeod, Z. Pan, W. Duan, C.M. Wang, Carbon nanotube–cement composites: a retrospect, IES J. Part A Civ. Struct. Eng. 4 (4) (2011) 254–265, https://doi.org/10.1080/19373260.2011.615474.

[65] S. Parveen, S. Rana, R. Fangueiro, A review on nanomaterial dispersion, microstructure, and mechanical properties of carbon nanotube and nanofiber reinforced cementitious composites, J. Nanomater. 2013 (2013), 710175, https://doi.org/10.1155/2013/710175.

[66] D. Han, R.D. Ferron, Influence of high mixing intensity on rheology, hydration, and microstructure of fresh state cement paste, Cement Concr. Res. 84 (2016) 95–106, https://doi.org/10.1016/j.cemconres.2016.03.004.

[67] E.S.R. Negim, N. Bekbayeva, L. Akmaral, U. Herki, B.M. Merey, N. Rinat, G. I Yeligbayeva, Effect of methyl cellulose/poly (acrylic acid) blends on physico-mechanical properties of Portland cement pastes, Orient. J. Chem. 33 (1) (2017) 450–457, https://doi.org/10.13005/ojc/330152.

[68] Y. Tian, X.-y. Jin, N.-g. Jin, R. Zhao, Z.-j. Li, H.-y. Ma, Research on the microstructure formation of polyacrylate latex modified mortars, Construct. Build. Mater. 47 (2013) 1381–1394, https://doi.org/10.1016/j.conbuildmat.2013.06.016.

[69] M. Alqedra, B. Dabbour, M. Arafa, Influence of several nano minerals on the mechanical properties of fresh and hardened concrete, Scientific Cooperations International Workshops on Engineering Branches 8 (2014) 9. August , Koc University, ISTANBUL/TURKEY, http://hdl.handle.net/20.500.12358/24552.

[70] H. Ma, Z. Li, Microstructures and mechanical properties of polymer modified mortars under distinct mechanisms, Construct. Build. Mater. 47 (2013) 579–587, https://doi.org/10.1016/j.conbuildmat.2013.05.048.

[71] H. Ma, Y. Tian, Z. Li, Interactions between organic and inorganic phases in PA-and PU/PA-modified-cement-based materials, J. Mater. Civ. Eng. 23 (10) (2011) 1412–1421, https://doi.org/10.1061/(ASCE)MT.1943-5533.0000302.

[72] R. Spragg, Y. Bu, K. Snyder, D. Bentz, J. Weiss, Electrical Testing of Cement-Based Materials: Role of Testing Techniques, Sample Conditioning, and Accelerated Curing, Indiana Department of Transportation and Purdue University, West Lafayette, Indiana, 2013, https://doi.org/10.5703/1288284315230. Publication FHWA/IN/JTRP-2013/28. Joint Transportation Research Program.

[73] A. D'Alessandro, C. Fabiani, A.L. Pisello, F. Ubertini, A.L. Materazzi, F. Cotana, Innovative concretes for low-carbon constructions: a review, Int. J. Low Carbon Technol. 12 (3) (2017) 289–309, https://doi.org/10.1093/ijlct/ctw013.

[74] S. Jiang, D. Zhou, L. Zhang, J. Ouyang, X. Yu, X. Cui, B. Han, Comparison of compressive strength and electrical resistivity of cementitious composites with different nano-and micro-fillers, Arch. Civ. Mech. Eng. 18 (2018) 60–68, https://doi.org/10.1016/j.acme.2017.05.010.

[75] G. Xiong, M. Deng, L. Xu, M. Tang, Properties of cement-based composites by doping nano-TiŌ 2, J. Chin. Ceram. Soc. 34 (9) (2006) 1158.

[76] I. Ismail, N. Bakar, T. Ling, N. Ideris, Z. Zain, N. Radacsi, Morphology and conductivity evaluation of electrospun polyacrylic acid (PAA) microfiber, Mater. Today: SAVE Proc. 17 (2019) 574–583, https://doi.org/10.1016/j.matpr.2019.06.337.

[77] D. LeonaviČIus, I.N.A. PundienĖ, J. PranckeviČIenĖ, G. Girskas, M. Kligys, The effect of the electrical conductivity of superplasticizers on the fluidity and early hydration parameters of cement paste, Ceram.–Silikáty 63 (4) (2019) 390–398, https://doi.org/10.13168/cs.2019.0035.

[78] L. Li, L. Liu, Y. Qing, Z. Zhang, N. Yan, Y. Wu, C. Tian, Stretchable alkaline poly (acrylic acid) electrolyte with high ionic conductivity enhanced by cellulose nanofibrils, Electrochim. Acta 270 (2018) 302–309, https://doi.org/10.1016/j.electacta.2018.03.088.

[79] J. Chen, C.-s. Poon, Photocatalytic cementitious materials: influence of the microstructure of cement paste on photocatalytic pollution degradation, Environ. Sci. Technol. 43 (23) (2009) 8948–8952, https://doi.org/10.1021/es902359n.

[80] M. Lackhoff, X. Prieto, N. Nestle, F. Dehn, R. Niessner, Photocatalytic activity of semiconductor-modified cement—influence of semiconductor type and cement ageing, Appl. Catal. B Environ. 43 (3) (2003) 205–216, https://doi.org/10.1016/S0926-3373(02)00303-X.

[81] C.S. Poon, E. Cheung, NO removal efficiency of photocatalytic paving blocks prepared with recycled materials, Construct. Build. Mater. 21 (8) (2007) 1746–1753, https://doi.org/10.1016/j.conbuildmat.2006.05.018.

[82] E. Jimenez-Relinque, J.R. Rodriguez-Garcia, A. Castillo, M. Castellote, Characteristics and efficiency of photocatalytic cementitious materials: type of binder, roughness and microstructure, Cement Concr. Res. 71 (2015) 124–131, https://doi.org/10.1016/j.cemconres.2015.02.003.

[83] G. Hüsken, H. Brouwers, Air Purification by Cementitious Materials: Evaluation of Air Purifying Properties, International Conference on Construction Building Technology, Kuala Lumpur, Malaysia, 2008.

[84] M.M. Ballari, Q. Yu, H. Brouwers, Experimental study of the NO and NO2 degradation by photocatalytically active concrete, Catal. Today 161 (1) (2011) 175–180, https://doi.org/10.1016/j.cattod.2010.09.028.